Wave–Particle Duality in Swirl–String Theory: Toroidal Circulation, Knot Collapse, and Photon-Induced Transitions

Omar Iskandarani
Independent Researcher, Groningen, The Netherlands

August 30, 2025

Abstract

We present a Swirl–String Theory (SST) interpretation of the electron's wave–particle duality based on Canon v0.3.1. The electron is modeled as a swirl-string admitting two phases: an unknotted, delocalized toroidal circulation $\mathcal{R}$ (wave-like) and a localized, knotted soliton (trefoil) $\mathcal{T}$ (particle-like). We define an effective energy functional including bulk swirl density, line tension, near-contact interactions, and helicity terms. Photon-induced transitions $\mathcal{R} \rightleftarrows \mathcal{T}$ occur at resonant frequencies determined by impedance matching between electromagnetic modes and topological excitations. We show how circulation quantization on $\mathcal{R}$ recovers de Broglie wave relations, while $\mathcal{T}$ provides a stable, localized excitation. This framework yields falsifiable predictions in atomic absorption spectra, Rydberg scaling, and polarization-dependent selection rules. Finally, we apply the formalism to the double slit experiment, explaining the coexistence of interference fringes and localized detection events.

1 Introduction

Wave–particle duality remains a central puzzle in quantum mechanics. The hydrodynamic representation of the Schrödinger equation by Madelung [1], the matter-wave hypothesis of de Broglie [2], and Bohm's hidden-variable interpretation [3, 4] all highlight fluid analogies. In superfluids, Onsager's circulation quantization [5] and Feynman's analysis of helium vortices [6] demonstrate how phase coherence enforces quantized flow. Earlier, Helmholtz [7] and Kelvin [8] established the conservation of vorticity and proposed atoms as vortex rings.

Within SST, the Canon postulates a universal swirl condensate with effective density and characteristic swirl velocity $\|\mathbf{v}_{\circlearrowleft}\|$. Electrons are interpreted not as point particles but as filamentary swirl-strings. We propose here that the dual character of the electron arises from two distinct phases of the same underlying string.

2 Two Phases of the Electron String

2.1 Unknotted toroidal ring $\mathcal{R}$

The delocalized phase is an unknotted ring circulation $\mathcal{R}$ with radius R and length $L(\mathcal{R}) = 2\pi R$. Its circulation is quantized:

$$\Gamma_n = \oint_{\mathcal{R}} \mathbf{v} \cdot d\boldsymbol{\ell} = n\frac{h}{m_e}, \qquad n \in \mathbb{Z}. \tag{1}$$

Hence the tangential speed is

$$v_\theta(R) = \frac{\Gamma_n}{2\pi R}, \tag{2}$$

and the phase around the ring is $e^{in\theta}$, yielding the de Broglie relation

$$\lambda_{\text{ring}} = \frac{2\pi R}{n} = \frac{h}{p_\theta}, \qquad p_\theta = m_e v_\theta. \tag{3}$$

Thus $\mathcal{R}$ naturally supports interference and standing-wave behavior.

2.2 Knotted trefoil soliton $\mathcal{T}$

The localized phase $\mathcal{T}$ is a knotted filament (e.g. trefoil 3_1) with enhanced curvature and helicity. Its invariants satisfy $C(\mathcal{T}) > 0$, $\mathcal{H}(\mathcal{T}) \neq 0$, and typically $L(\mathcal{T}) > L(\mathcal{R})$ for equal scale.

2.3 Effective energy functional

We postulate an effective energy functional

$$\boxed{\mathcal{E}_{\text{eff}}[K] = \underbrace{\epsilon_0 A L(K)}_{\text{bulk swirl energy}} + \underbrace{\beta L(K)}_{\text{line tension}} + \underbrace{\alpha C(K)}_{\text{near-contact}} + \underbrace{\gamma \mathcal{H}(K)}_{\text{helicity}}} \tag{4}$$

where K is the filament curve, $A = \pi r_c^2$ is the core cross-sectional area, and ϵ_0 is the Canon bulk energy density

$$\epsilon_0 = \frac{4}{\alpha_{\text{fs}}\, \varphi} \left(\tfrac{1}{2}\|\mathbf{v}_{\circlearrowleft}\|^2\right). \tag{5}$$

2.4 Dimensional analysis

- $[\epsilon_0] = \mathrm{J\,m^{-3}}$, $[A] = \mathrm{m^2}$, $[L] = \mathrm{m} \Rightarrow [\epsilon_0 A L] = \mathrm{J}$.
- $[\beta] = \mathrm{J\,m^{-1}}$, hence $[\beta L] = \mathrm{J}$.
- αC, $\gamma \mathcal{H}$ contribute as energy terms.

Numerically, with Canon constants,

$$\epsilon_0 \approx 1.4187 \times 10^8\ \mathrm{J\,m^{-3}}, \quad A \approx 6.24 \times 10^{-30}\ \mathrm{m^2}, \tag{6}$$

so bulk energy per length is

$$\epsilon_0 A \approx 8.85 \times 10^{-22}\ \mathrm{J\,m^{-1}}. \tag{7}$$

3 Photon-Driven Transitions

3.1 Resonance condition

The transition $\mathcal{R} \to \mathcal{T}$ changes the energy by

$$\Delta E = (\epsilon_0 A + \beta)\Delta L + \alpha C(\mathcal{T}) + \gamma \mathcal{H}(\mathcal{T}). \tag{8}$$

Resonance occurs when

$$\boxed{\hbar\omega \approx \Delta E}. \tag{9}$$

3.2 Selection rules

- Angular momentum matching: photon helicity must match the winding number (e.g. $\Delta n = \pm 3$ for trefoil).
- Radius dependence: larger R reduces ΔL, lowering resonance energy (Rydberg scaling).
- Polarization dependence: circular polarization aligned with knot chirality enhances coupling.

4 Effective Field Theory Formulation

At the EFT level, the string world-sheet Σ enters a Lagrangian

$$\mathcal{L} = \tfrac{1}{2}\|\mathbf{v}\|^2 - \rho_E - \beta\ell[\Sigma] - \alpha\mathcal{C}[\Sigma] - \gamma\mathcal{H}[\Sigma] + \mathcal{L}^{\text{int}}_{\text{EM}}[A_\mu;\Sigma]. \tag{10}$$

In the static limit, $\mathcal{L} \to -\mathcal{E}_{\text{eff}}$. Time-dependent solutions yield Rabi-like oscillations between $\mathcal{R}$ and $\mathcal{T}$ under monochromatic drive $\omega \approx \Delta E/\hbar$.

5 Predictions and Tests

1. **Spectral lines:** new resonances in absorption spectra, not coinciding with standard atomic transitions.
2. **Rydberg atoms:** red-shifted knotting lines with increasing principal quantum number.
3. **Pump–probe:** suppression of interference fringes coincident with localization after resonant pump.
4. **Polarization dependence:** transition rates sensitive to photon chirality.

6 Application: Double Slit Experiment

The SST picture explains the double slit experiment by assigning the two phases $\mathcal{R}$ and $\mathcal{T}$ distinct roles.

6.1 Propagation as delocalized circulation

Prior to detection, the electron is in the $\mathcal{R}$ phase: a toroidal circulation with quantized phase $e^{in\theta}$. When encountering two slits, the circulation bifurcates into two coherent streams, producing downstream

$$\Psi(x) = \Psi_1(x) + \Psi_2(x), \tag{11}$$

so that the observed intensity is

$$I(x) \propto |\Psi_1(x) + \Psi_2(x)|^2, \tag{12}$$

yielding interference fringes.

6.2 Detection as knot collapse

At the detection screen, the swirl string collapses into the knotted soliton $\mathcal{T}$, producing a *localized* impact. Thus interference and localization coexist:

$$\boxed{\text{Propagation: } \mathcal{R} \text{ (wave)}; \quad \textit{Detection} : \mathcal{T} \text{ (particle)}.} \tag{13}$$

6.3 Which-slit measurements

If one slit is monitored by a detector, photon interaction forces premature collapse $\mathcal{R} \to \mathcal{T}$ before interference can occur. Hence fringes vanish when which-slit information is obtained.

6.4 Dimensional consistency

The Canon bulk energy per unit length is

$$\epsilon_0 A \approx 8.85 \times 10^{-22} \text{ J/m},$$

far smaller than photon interaction energies ($\sim 10^{-19}$ J at visible frequencies), so even weak monitoring collapses the circulation, explaining measurement-induced loss of interference.

7 Conclusion

In SST, the same electron string supports both a delocalized circulation $\mathcal{R}$ (wave aspect) and a localized knot $\mathcal{T}$ (particle aspect). Photon-induced transitions between these phases provide a dynamical explanation of wave–particle duality consistent with the Canon and hydrodynamic analogies. The application to the double slit experiment demonstrates how interference patterns and localized detection events arise from the same underlying string dynamics.

Appendix: Popular Summary

A swirl-ring can ripple smoothly like a hula-hoop (wave). If twisted into a knot, the swirl bunches up in one spot (particle). A photon of just the right frequency can flip the string between these two states. In the double slit experiment, the hula-hoop can pass through both slits at once, but when it hits the wall, it snaps into a knot at one spot.

A Quantitative Fringe Geometry and Visibility

Consider a double slit with center-to-center separation s and distance L from slits to screen. Let the electron approach in the delocalized ring phase $\mathcal{R}$ with mean axial momentum p_z (de Broglie wavelength $\lambda = h/p_z$). In the Fraunhofer regime ($L \gg s^2/\lambda$), the transverse intensity on the screen is well approximated by

$$I(x) \;\propto\; I_1(x) + I_2(x) + 2\sqrt{I_1(x) I_2(x)}\,\cos\!\Big(\tfrac{2\pi s}{\lambda}\,\tfrac{x}{L} + \phi_0\Big), \tag{14}$$

with fringe spacing

$$\boxed{\; d \;=\; \frac{\lambda L}{s} \;}. \tag{15}$$

Within SST, the phase ϕ_0 is the circulation phase offset inherited from $\mathcal{R}$; any path-dependent coupling to the environment adds a random phase $\delta\phi$ that reduces the fringe visibility

$$\mathcal{V} \equiv \frac{I_{\max} - I_{\min}}{I_{\max} + I_{\min}} \;=\; \big|\langle e^{i\delta\phi}\rangle\big|. \tag{16}$$

A.1 Ring-phase mapping

For the ring state $\mathcal{R}$ with quantized azimuthal phase $e^{in\theta}$, the two slits act as partial projectors of this phase onto two spatially separated downstream wavefronts. The resulting interference encodes the *same* azimuthal winding through the optical path difference $\Delta\ell(x) \approx s\,x/L$, hence the cosine argument above.

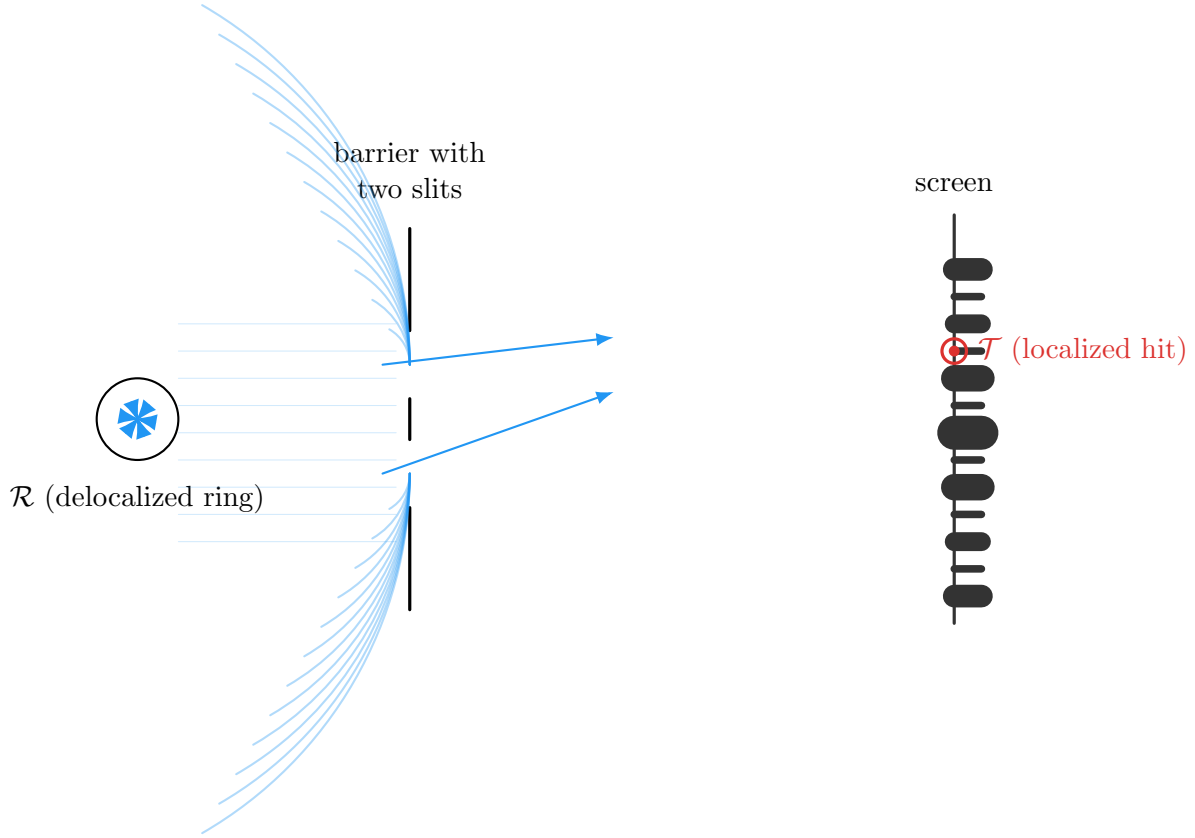

Figure 1: SST double slit schematic. The electron approaches as a delocalized toroidal circulation $\mathcal{R}$ (ring), whose phase bifurcates at two slits to produce coherent downstream fields that interfere. At the screen, interaction triggers collapse into a localized knotted state $\mathcal{T}$, yielding discrete impacts while the ensemble reproduces the fringe intensity.

B Which-Way Coupling and Decoherence in SST

In SST language, "which-way" monitoring is an *EM impedance* to the ring phase, parameterized by a coupling rate Γ (net photon or field-interaction rate that carries path information). Let τ be the transit time through the interferometer. For weak, memoryless monitoring the phase undergoes a random walk, giving the standard exponential visibility law [**?**]

$$\boxed{\mathcal{V}(\Gamma, \tau) \;=\; e^{-\Gamma\tau}}. \tag{17}$$

Equivalently, define a *monitoring strength* $\eta \in [0, 1]$ as the single-pass which-way information; then $\mathcal{V} = \sqrt{1-\eta}$ (two-outcome, information-balance form). Both parameterizations are compatible at small η via $\eta \simeq 2(1 - e^{-\Gamma\tau})$.

SST mechanism. Microscopically, the EM coupling stochastically seeds premature $\mathcal{R} \to \mathcal{T}$ collapses *upstream*, terminating coherent superposition. Equation (17) thus measures the survival probability of coherence before the knotting transition.

B.1 Dimensional check

Γ has units s^{-1} and τ has units s, so $\Gamma\tau$ is dimensionless, consistent with (17).

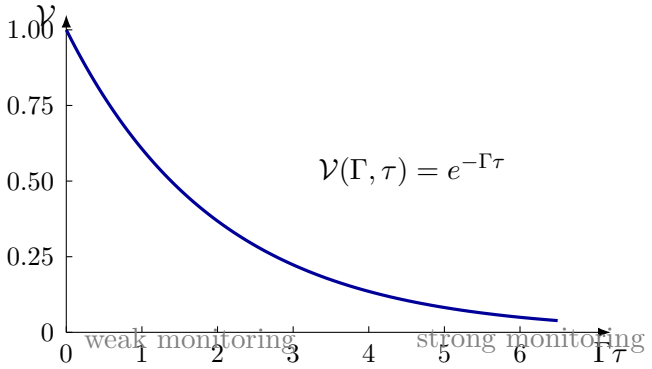

Figure 2: Fringe visibility vs. which-way coupling in SST. The parameter Γ encodes EM impedance to the $\mathcal{R}$ phase (path information rate), τ is the transit time. Exponential decay of visibility reflects coherence loss prior to recombination.

C Delayed-Choice and Quantum Eraser (SST View)

In a Wheeler-type delayed choice, the interferometer is reconfigured *after* the electron passes the slits [**?**]. In SST, this reconfiguration alters whether the downstream optics *allow* continued $\mathcal{R}$-phase recombination or instead force local $\mathcal{T}$-phase collapse:

- **Interference mode on:** downstream optics preserve the $\mathcal{R}$ phase coherence until the screen $\Rightarrow$ fringes.
- **Which-way mode on:** downstream optics couple EM impedance strongly, enforcing premature $\mathcal{R}\to\mathcal{T}$ collapse $\Rightarrow$ no fringes.

A quantum eraser removes the stored which-way information, effectively *post-selecting* runs where $\mathcal{R}$-coherence survived to the recombination stage; sorted sub-ensembles then display fringes.

D Spectroscopic Rabi Drive Between $\mathcal{R}$ and $\mathcal{T}$

We model the $\mathcal{R} \leftrightarrow \mathcal{T}$ manifold as a driven two-level system with detuning $\Delta = \omega - \omega_0$ (where $\hbar\omega_0 = \Delta E_{\mathcal{R}\to\mathcal{T}}$) and coupling Ω_R set by the EM impedance overlap:

$$\dot{c}_{\mathcal{R}} = -\tfrac{i}{2}\Omega_R c_{\mathcal{T}} - \tfrac{\gamma_{\mathcal{R}}}{2} c_{\mathcal{R}}, \tag{18}$$

$$\dot{c}_{\mathcal{T}} = -\tfrac{i}{2}\Omega_R c_{\mathcal{R}} - \Big(\tfrac{\gamma_{\mathcal{T}}}{2} + i\Delta\Big) c_{\mathcal{T}}. \tag{19}$$

At resonance ($\Delta = 0$) and for $\gamma_{\mathcal{R}}, \gamma_{\mathcal{T}} \ll \Omega_R$,

$$P_{\mathcal{T}}(t) = |c_{\mathcal{T}}(t)|^2 \;=\; \sin^2\Big(\frac{\Omega_R t}{2}\Big)\, e^{-\gamma t}, \qquad \gamma \equiv \tfrac{\gamma_{\mathcal{R}}+\gamma_{\mathcal{T}}}{2}. \tag{20}$$

A *pump–probe* synchronized to the flight time across the interferometer can therefore *gate* the knotting probability and modulate fringe visibility in a time-resolved fashion.

Boxed Result (SST double slit). An electron is a single swirl-string with two phases: $\mathcal{R}$ (delocalized ring) for propagation and $\mathcal{T}$ (knotted soliton) for detection. Interference arises from coherent splitting and recombination of $\mathcal{R}$; localized impacts result from $\mathcal{R} \to \mathcal{T}$ collapse at the screen. Which-way monitoring increases the EM impedance, raising the premature knotting rate Γ; the fringe visibility obeys $\mathcal{V} = e^{-\Gamma\tau}$ and vanishes in the strong-monitoring limit.

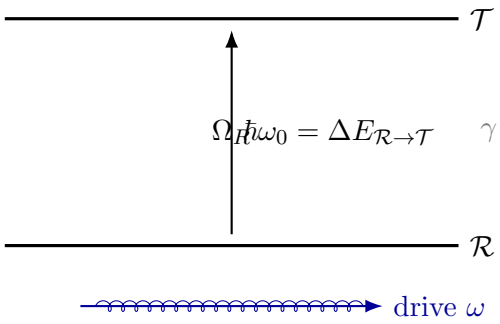

Figure 3: Two-level SST manifold for $\mathcal{R} \leftrightarrow \mathcal{T}$ with Rabi drive. At resonance $\omega = \omega_0$, the knotting probability oscillates at Ω_R and decays at rate γ, enabling pump–probe control of collapse within an interferometer.

References

[1] E. Madelung. Quantentheorie in hydrodynamischer Form. *Zeitschrift für Physik*, 40:322–326, 1927. doi:10.1007/BF01400372.

[2] L. de Broglie. Recherches sur la théorie des quanta. *Annales de Physique*, 3(10):22–128, 1925. doi:10.1051/anphys/192510030022.

[3] D. Bohm. A Suggested Interpretation of the Quantum Theory in Terms of "Hidden" Variables I. *Phys. Rev.*, 85(2):166–179, 1952. doi:10.1103/PhysRev.85.166.

[4] D. Bohm. A Suggested Interpretation of the Quantum Theory in Terms of "Hidden" Variables II. *Phys. Rev.*, 85(2):180–193, 1952. doi:10.1103/PhysRev.85.180.

[5] L. Onsager. Statistical hydrodynamics. *Il Nuovo Cimento (Supplemento)*, 6:279–287, 1949. doi:10.1007/BF02780991.

[6] R. P. Feynman. Application of Quantum Mechanics to Liquid Helium. In C. J. Gorter, editor, *Progress in Low Temperature Physics, Vol. I*, pages 17–53. North-Holland, 1955. doi:10.1016/S0079-6417(08)60077-3.

[7] H. von Helmholtz. Über Integrale der hydrodynamischen Gleichungen, welche den Wirbelbewegungen entsprechen. *Journal für die reine und angewandte Mathematik*, 55:25–55, 1858. doi:10.1515/crll.1858.55.25.

[8] W. Thomson (Lord Kelvin). On Vortex Motion. *Transactions of the Royal Society of Edinburgh*, 25:217–260, 1869.